

A NEW FIELD LINE ADVECTION MODEL FOR SOLAR PARTICLE ACCELERATION

I. V. SOKOLOV,¹ I. I. ROUSSEV,¹ T. I. GOMBOSI,¹ M. A. LEE,² J. KÓTA,³
T. G. FORBES,² W. B. MANCHESTER,¹ AND J. I. SAKAI⁴

Received 2004 June 25; accepted 2004 October 18; published 2004 October 27

ABSTRACT

The diffusive acceleration of solar protons at a shock wave driven by a realistic coronal mass ejection is modeled using a new field line advection model for particle acceleration coupled with a global MHD code. The new model described in this Letter includes effects important for the particle acceleration and transport, by means of diffusive shock acceleration, and employs Lagrangian meshes. We performed a frequent dynamical coupling between two numerical codes in order to account for the time-dependent history of an evolving shock wave driven by a solar eruption. The numerical results discussed here demonstrate that this mechanism can account for the production of high-energy solar protons observed during the early stages of gradual events.

Subject headings: acceleration of particles — MHD — shock waves — Sun: coronal mass ejections (CMEs) — Sun: magnetic fields

Online material: mpeg animation

1. INTRODUCTION

The solar energetic particle (SEP) events associated with coronal mass ejections (CMEs) are of particular importance for space weather because they endanger human life in outer space and pose major hazards for spacecraft in the solar system. High-energy solar protons (>100 MeV) can be accelerated within a short period of time (≤ 1 hr) after the initiation of solar eruptions, which makes them difficult to predict, and pose a serious concern for the design and operation of both manned and unmanned space missions. Recent theories and related observations (e.g., Cliver et al. 2004; Kahler 1994; Lee 1983; Li et al. 2003; Ng et al. 1999, 2003; Zank et al. 2000) suggest that these high-energy particles are the result of the first-order Fermi acceleration process (Fermi 1949) at a shock wave driven by a solar eruption, the so-called diffusive shock acceleration (DSA), in the Sun's proximity ($2\text{--}15 R_{\odot}$). These theories, however, have been debated within the community (e.g., Bulanov & Sokolov 1984; Reames 1999, 2002; Tylka 2001) because very little is known about the dynamical properties of CME-driven shock waves in the inner corona soon after the onset of the eruption and whether or not the level of turbulence at the shock is sufficient for this mechanism to work.

To address the problem of shock wave generation, we constructed a fully three-dimensional MHD model of a CME that incorporates solar magnetogram data and a loss-of-equilibrium mechanism (Roussev et al. 2004). We demonstrated that a CME-driven shock wave can develop close to the Sun ($\sim 4 R_{\odot}$) and is of a strength sufficiently high to have accelerated SEPs during the solar eruptive event that took place on 1998 May 2 in NOAA Active Region 8210. In this Letter, we extend that previous study by using a new field line advection model for particle acceleration (FLAMPA), coupled with a global MHD

code, BATS-R-US (Block Adaptive-Tree Solar-wind Roe-type Upwind Scheme; Powell et al. 1999). Previous models of particle acceleration at CME-driven shocks, by means of DSA, employed either an idealized, spherically symmetric shock wave (Li et al. 2003; Zank et al. 2000) or one taken from a snapshot of the compressible MHD simulation of a CME event (Heras et al. 1995; J. Kóta et al. 2004, in preparation) and extended it in time assuming self-similarity of the flow. Here, we take a different approach and follow the time-dependent, three-dimensional evolution of a shock wave as we advance the distribution of solar protons in time, subject to DSA. For this purpose, we perform frequent dynamical coupling between BATS-R-US and FLAMPA, so that we capture timescales and spatial gradients of dynamical importance for the DSA of solar protons. The results of our coupled SEP-MHD simulation discussed here clearly demonstrate the capability to provide a high-performance simulation of the acceleration and transport of solar protons observed during the early stages of gradual SEP events.

2. DESCRIPTION OF FLAMPA

The complexity of any kinetic theory for SEPs, in the case of an arbitrary geometry, results from the requirement to solve an equation with a dimensionality greater than three; the canonical distribution function of particles, f , depends on three spatial x_i and, at least, one momentum $p = |\mathbf{p}|$ coordinate, as well as time, t . In order to handle this problem in our new field line advection model for particle acceleration, we assume that the particle motion in physical space consists primarily of diffusion along the magnetic field, \mathbf{B} , and advection with plasma into which the magnetic field is frozen. With these assumptions, the governing kinetic equation for particle transport is reducible to a spatially one-dimensional equation with respect to the coordinate, s , measuring distance along the magnetic field. Here s is such that $\partial/\partial s = \mathbf{b} \cdot \nabla$, where $\mathbf{b} = \mathbf{B}/|\mathbf{B}|$ and $\nabla = \partial/\partial x_i$. To accomplish this, we use the Lagrangian coordinates (Landau & Lifshitz 1959), thus allowing us to fully account for the advection of both SEPs and the frozen-in magnetic field with the flow. As a result, FLAMPA reduces the multidimensional problem to a simple one-dimensional one with no loss of generality.

The method described below works for several possible

¹ Center for Space Environment Modeling, University of Michigan at Ann Arbor, 2455 Hayward Street, Ann Arbor, MI 48109; igorsok@umich.edu, iroussev@umich.edu, tamas@umich.edu, chipm@umich.edu.

² Department of Physics and Institute for the Study of Earth, Ocean, and Space, University of New Hampshire, Durham, NH 03824; marty.lee@unh.edu, terry.forbes@unh.edu.

³ Lunar and Planetary Laboratory, University of Arizona, 1629 East University Boulevard, Tucson, AZ 85721-0092; kota@lpl.arizona.edu.

⁴ Laboratory for Plasma Astrophysics, Faculty of Engineering, Toyama University, Toyama 930-8555, Japan; sakaijun@eng.toyama-u.ac.jp.

choices of kinetic equation, like the Boltzmann equation for the transport of charged particles with a gyrotropic distribution function (Isenberg 1997; Li et al. 2003; Skilling 1971). Here, as a simpler example, we demonstrate how the method works for the standard cosmic-ray transport equation in the DSA limit:

$$\frac{\partial f}{\partial t} + (\mathbf{u} \cdot \nabla) f - \frac{1}{3} (\nabla \cdot \mathbf{u}) \frac{\partial f}{\partial \ln p} = \nabla \cdot (\mathbf{D} \cdot \nabla f), \quad (1)$$

for the isotropic part $f(x_i, p, t)$ of the canonical distribution function. This equation is averaged with respect to the gyro-phase and pitch angle, μ , of particle motion about the magnetic field. Here \mathbf{u} is the velocity field, and \mathbf{D} is the diffusion tensor along the magnetic field: $\mathbf{D} = D\mathbf{b} \otimes \mathbf{b}$, with D being a scalar diffusion coefficient.

With the use of Lagrangian coordinates, and assuming that the magnetic field is ideally frozen into the plasma, we dictate that a given field line consists of the same set of Lagrangian meshes at any instant of time. By using the Lagrangian time derivative, $d/dt = \partial/\partial t + \mathbf{u} \cdot \nabla$, and employing the solenoidal constraint, $\nabla \cdot \mathbf{B} = 0$, as well as the continuity equation, $\nabla \cdot \mathbf{u} = -d \ln \rho/dt$, one can transform equation (1) into a one-dimensional equation:

$$\frac{df}{dt} + \frac{1}{3} \frac{d \ln \rho}{dt} \frac{\partial f}{\partial \ln p} = B \frac{\partial}{\partial s} \left(\frac{D}{B} \frac{\partial f}{\partial s} \right). \quad (2)$$

The term on the right-hand side of equation (2) combines the effects of spatial diffusion along the magnetic field and adiabatic focusing due to spatial gradients in B . In order to solve this equation, with $\rho(s, t)$ and $B(s, t)$ taken from the MHD model, we need to specify the diffusion coefficient, D , and the boundary condition at some injection energy.

To address the injection energy problem in our model, we assume a suprathermal tail of protons from the thermal distribution at the local kinetic temperature T_p (~ 0.3 keV at the Sun), through to the injection energy, $E_{\text{inj}} = p_{\text{inj}}^2/(2m_p) = 10$ keV. We consider the suprathermal differential intensity ($\propto f p^2$) to depend on the energy, E , as $E^{-3/2}$, and to be proportional to $N_p = \rho/m_p$ (where m_p is the proton mass). Specifically, the canonical distribution function at $p = p_{\text{inj}}$ is chosen as

$$f|_{p=p_{\text{inj}}} = \frac{c_{\text{inj}}}{8\pi} \frac{N_p}{(2m_p T_p)^{3/2}} \left(\frac{\sqrt{2m_p T_p}}{p_{\text{inj}}} \right)^5, \quad (3)$$

where the unknown injection efficiency, c_{inj} ($\sim 3.4 \times 10^{-4}$), determines the absolute value of the computed SEP flux.

Assume an irregular magnetic field, δB , that is self-excited by the fast particles with the spectrum $f p^2 \sim E^{-3/2}$. We find that the spectrum of turbulence $I(k)$ scales with the wavenumber, k , as $I(k) = (\delta B)^2/(\pi|k|)$. The quantity $(\delta B)^2$ is of the order of the local value of the turbulent energy density. Following Lee (1983), one can express $(\delta B/B)_{\text{sh}}^2$ at the shock front as $\text{const } c_{\text{inj}} M_A \approx 0.2 M_A$ (where M_A is the Alfvén Mach number of the shock wave). The spatial diffusion coefficient, D , can be derived in the usual manner from the scattering integral with

respect to particle pitch angle, $\partial_\mu (D_{\mu\mu} \partial_\mu f)$, with $D_{\mu\mu}$ adopted from Lee (1983):

$$D = \frac{v^2}{8} \int_{-1}^1 \frac{(1 - \mu^2)^2}{D_{\mu\mu}} d\mu, \quad D_{\mu\mu} = \frac{\pi e^2 (1 - \mu^2) v}{2c^2 |\mu| p^2} I \frac{eB}{c p \mu}.$$

Here v , e , and c are the proton speed, electric charge, and speed of light, respectively. Solving the integral, one gets

$$D = \frac{1}{3} \lambda_{\parallel} v = \frac{1}{3} \left(\frac{B}{\delta B} \right)^2 r_B v, \quad (4)$$

where $r_B = cp/(eB)$ is the Larmor radius and $\lambda_{\parallel} = r_B (B/\delta B)^2$ is the mean free path of particles along the magnetic field. Behind the shock wave (for $R_{\odot} < R < 0.9R_{\text{sh}}$, with R_{sh} being the shock location), we assume a decaying level of turbulence and adopt $(\delta B/B)^2 = (\delta B/B)_{\text{sh}}^2 R/(0.9R_{\text{sh}})$. Upstream of the shock wave there is free streaming of particles; thus, we use a different formula for λ_{\parallel} . Following Li et al. (2003), we assume a spatial dependence of $\lambda_{\parallel} \propto R$. Specifically, we assume that $D \sim 0.1$ [AU] $v(p c/1$ [GeV]) $^{1/3} (R/1$ [AU]). In order to compensate for the eroded width of the shock front due to the finite mesh size in the MHD calculations ($\sim 0.1 R_{\odot}$), the diffusion coefficient for low-energy particles is artificially enhanced according to $D = \max\{D, D_{\text{min}}\}$, where $D_{\text{min}} = 0.1 R_{\odot} \times 10^5 \text{ m s}^{-1} = 7.0 \times 10^{12} \text{ m}^2 \text{ s}^{-1}$.

The FLAMPA code is designed to integrate equation (2) numerically, with a spatial diffusion coefficient prescribed by equation (4), and using equation (3) as a boundary condition at the injection energy. The advection of particles with respect to the momentum coordinate ($\propto \partial f/\partial \ln p$) is solved by using an explicit, second-order accurate upwind scheme. The integration limits are set to p_{inj} and $p_{\text{max}} = 10$ GeV/ c . The discretization is done in 200 equally spaced grid points, p_i , with respect to $\ln p$. The spatial diffusion of particles and their adiabatic focusing ($\propto \partial_s [(D/B) \partial_s f]$) are treated using an implicit alternate direction of integration scheme.

3. COUPLING BETWEEN BATS-R-US AND FLAMPA

To power up the SEP model, we are required to couple FLAMPA with the global MHD code. To do this, we need to trace initially a particular field line; set the Lagrangian meshes along this field line; follow the Lagrangian meshes in time; and extract the MHD parameters (ρ , B , and T_p) that are needed for FLAMPA.

At time instant t_0 (before the shock wave forms), we trace a given field line from a starting point $\mathbf{x}_0 = \{-29.95, 0, -12.20\} R_{\odot}$ all the way back to the Sun. This field line is then extended out to 1 AU, and the MHD variables are extrapolated using the steady state MHD solution for the inner heliosphere region. The field line tracing is done by integrating the following differential equation describing the field line position: $d\mathbf{x} = \mathbf{b} ds$, using \mathbf{x}_0 as a boundary condition. The values of \mathbf{b} are taken from the MHD simulation of Roussev et al. (2004). For $t > t_0$, we trace the *same* field line by following the Lagrangian meshes it consists of: \mathbf{x}_n ($0 \leq n \leq L_s$ and $L_s \sim 1500$). To accomplish this, we solve L_s time-dependent equations of the kind $dx_n/dt = \mathbf{u}(\mathbf{x}_n, t)$, with a velocity field \mathbf{u} taken from the MHD solution at each time step. The left panel in Figure 1 shows the time evolution of the field line traced in our calculations, whereas the right panel provides a time sequence of mass density profiles extracted along this field

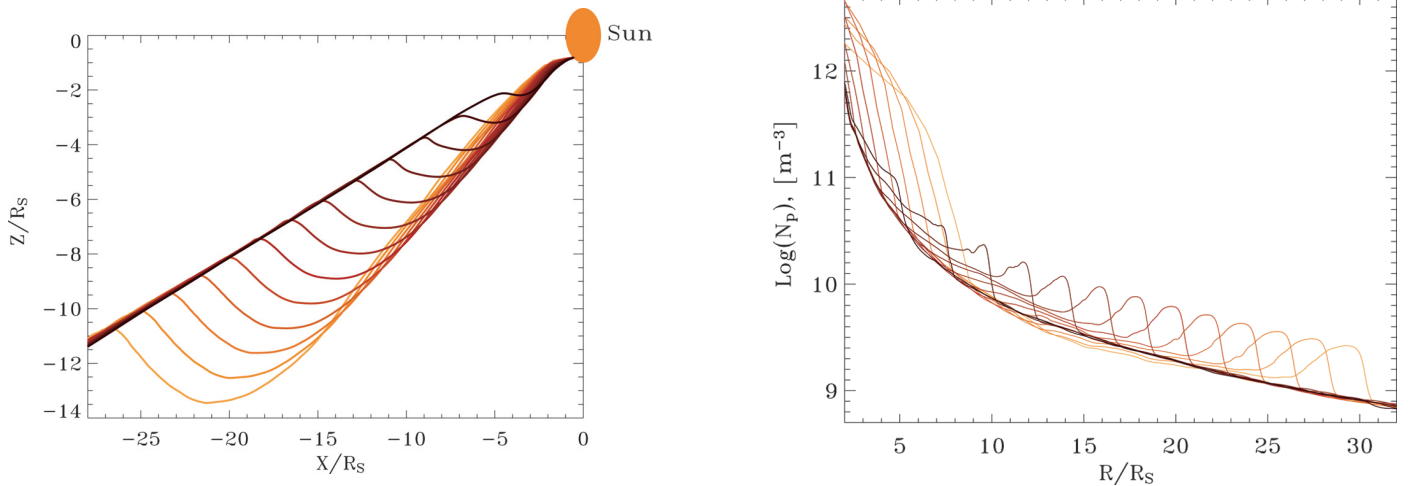


FIG. 1.—*Left*: Time sequence showing the evolution of the traced magnetic field line used to couple BATS-R-US with FLAMPA. The time interval between two adjacent curves is 30 minutes. The whole sequence spans a time interval of 6 hr. *Right*: Time sequence of profiles of the proton number density extracted along the evolving magnetic field line from the left panel.

line. The temporal evolution of the shock wave can be assessed from this figure.

After performing a code coupling at some time instant t_1 , we allow the shock wave in the MHD solution to travel the distance ds between two neighboring Lagrangian meshes. At this time instant, t_2 ($\leq t_1 + 60$ s), we do the next coupling between BATS-R-US and FLAMPA. In essence, we extract the updated values of the magnetic field strength B , temperature T_p , and proton number density N_p along the traced field line (all taken from the MHD simulation) and send those as an input to FLAMPA. We also need to find the shock wave front in the discrete MHD data set and to sharpen the density profile near it, because in reality this front is sharper than that in the MHD simulations. The Lagrangian derivative $d \ln \rho / dt$ is computed from $\ln [N_p(t_2)/N_p(t_1)] / (t_2 - t_1)$. The particle distribution function, $f(\mathbf{x}_n, p_i)$, is then updated from t_1 to t_2 , using the solution algorithms described above.

4. DISCUSSION OF NUMERICAL RESULTS

As described in our previous study, the CME becomes supersonic with respect to the local fast-wave speed about $t_1 = 0.5$ hr after the onset of the eruption (this corresponds to a simulation time of 2.4 hr; for details, we refer to Fig. 2 from Roussev et al. 2004). At this time, a shock wave forms that reaches a compression ratio of about 3 by the time it has traveled a radial distance $r \approx 6$ (in units of solar radius) from the surface. For this shock's compression ratio, the theory of DSA predicts a spectral index of nonrelativistic protons of 1.25. Note that while in the previous study, the shock parameters were extracted along a static straight line, here we follow the shock evolution along a moving magnetic field line. Thus, some differences in the shock evolution are to be expected.

With the input from the MHD code, the FLAMPA code computes the diffusive acceleration of solar protons at the shock front as it evolves. The left panel in Figure 2 illustrates a snapshot

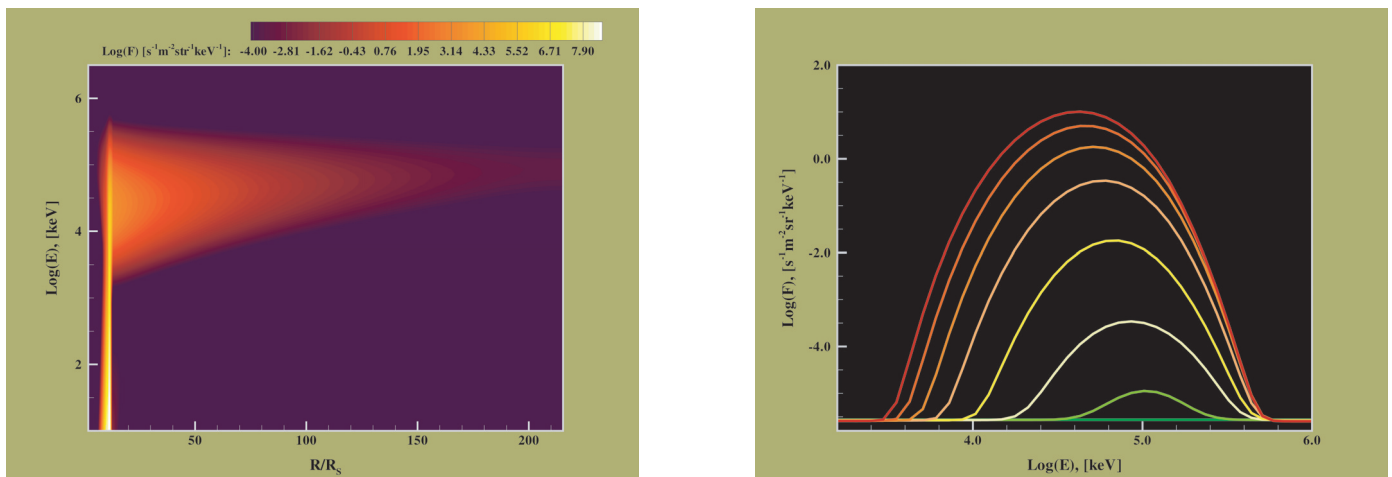


FIG. 2.—*Left*: Snapshot of the differential proton intensity, $F(r, E)$, at $t = t_1 + 1.6$ hr (t_1 being the shock formation time). The shock wave is located at $r = 12.2$ at this time. This figure is also available as an mpeg animation in the electronic edition of the *Astrophysical Journal*. *Right*: Time sequence of spectra of the differential proton intensity at distance $r = 215.5$ (1 AU). The time interval between two adjacent curves is 30 minutes. The low-lying dark green curve corresponds to $t = t_1$, whereas the dark red curve refers to $t = t_1 + 3.5$ hr (when the shock is at $r = 20.3$).

of the differential proton intensity, $F(r, E) \propto fp^2(E)$, at the time when the shock wave is at $r = 12.2$. A time sequence of spectra of F at radial distance $r = 215.5$ (1 AU) is shown in the right panel of this figure. Both panels in Figure 2 demonstrate key features predicted from the theory of DSA, namely, the existence of an exponential tail of particles upstream of the shock wave (the length of the tail is $\sim D/u_{\text{sh}}$, where u_{sh} is the shock speed); elevated proton intensities at high energies behind the shock wave; and escape of high-energy (>1 MeV) particles upstream of the shock wave. The latter is due to the fact that $D \propto E$, meaning that once the particles are accelerated to sufficiently high energies, their upstream tail becomes very large [$D/u_{\text{sh}} \gg u_{\text{sh}}(t - t_1)$]. Thus, they avoid any further diffusive acceleration at the shock front. These are the particles of particular importance for space weather, and they are the ones considered as precursors of disruptive events in the near-Earth environment.

In the proximity of the shock wave, the energy spectrum of protons is hard ($\Gamma \sim 1.3$) in the range from 10 keV through to ~ 10 MeV, and then it softens at higher energies (≤ 700 MeV). The cutoff energy in the spectrum grows very rapidly at first [$\propto u_{\text{sh}}^2(t - t_1)B$], reaches a maximum value of about 700 MeV when the shock is at nearly $r = 15$, and then gradually starts declining as the field strength in the upstream region falls off with distance from the Sun. The energy cutoff is down to 450 MeV when the shock wave is at $r = 30$.

5. CONCLUSIONS AND FUTURE WORK

The new model presented in this Letter, FLAMPA, has been developed to simulate the time-dependent transport and diffusive acceleration of particles at shock waves driven by CMEs. That is, FLAMPA implements the theory of DSA into a state-of-the-art numerical code. This code has been coupled with the BATS-R-US code that solves the equations of compressible MHD in three-dimensional, block-adaptive grid geometry. Within the framework of this coupling, we followed the complete time-dependent history of a realistic shock wave driven by a solar eruption, and we simulated the effects of particle transport and diffusive acceleration as the shock wave evolves

in the region from 4 to 30 R_{\odot} . The results of this numerical investigation demonstrate that the theory of DSA alone can account for the production of high-energy protons during solar eruptions. While in the previous study (Roussev et al. 2004) we provided only an upper limit of the cutoff energy of solar protons, here we quantify the actual energy spectrum of protons. FLAMPA is a powerful tool that can be used with any realistic CME model to probe the means of particle acceleration at CME-driven shocks. The computed proton intensities can be tested against those observed at the Earth.

By comparing the simulation results at 1 AU with the available SEP data for the 1998 May 2 event (proton fluxes from GOES-8 satellite), with a choice of $c_{\text{inj}} = 3.4 \times 10^{-4}$ we find good agreement for six of the energy channels (>5 , >10 , >30 , >50 , >60 , and >100 MeV) and a slightly worse agreement for the “ >1 MeV” channel. The onset of the observed SEP event happens ~ 30 – 60 minutes after the onset of the flare (Danilova et al. 1999), while in our simulation this occurs ~ 30 minutes after the shock wave forms (or ~ 60 minutes after the onset of the eruption). We conclude that what is important to know from the CME model is when (or if) the shock wave forms on the magnetic field line connecting the Sun with the Earth. This proves that our coupled model is very informative, and it allows us to use real SEP data to verify it.

In future investigations, we will include a realistic model of turbulence in FLAMPA that accounts for the local wave generation by energetic ions and wave damping (e.g., Giacalone & Jokipii 1994; Ng et al. 1999, 2003) and related second-order Fermi acceleration. Although many potentially significant effects remain to be investigated, FLAMPA already incorporates much of the fundamental physics that is necessary to probe the nature of gradual SEP events associated with solar eruptions.

The authors thank J. Giacalone, J. R. Jokipii, C. Ng, A. Tylka, and an unknown referee for their comments. This research work was supported by the following grants: DoD MURI F49620-01-1-0359, NSF ACI-9876943, NSF ATM-0325332, NASA NAG5-9406, 11797, 10977, and 10852, NSF ATM-0091527, and NSF ATM-0327512.

REFERENCES

- Bulanov, S. V., & Sokolov, I. V. 1984, *Soviet Astron. Lett.*, 10, 247
 Cliver, E. W., Kahler, S. W., & Reames, D. V. 2004, *ApJ*, 605, 902
 Danilova, O. A., et al. 1999, *Proc. 26th Int. Cosmic Ray Conf. (Salt Lake City)*, 6, 399
 Fermi, E. 1949, *Phys. Rev.*, 75, 1169
 Giacalone, J., & Jokipii, J. R. 1994, *ApJ*, 430, L137
 Heras, A. M., et al. 1995, *ApJ*, 445, 497
 Isenberg, P. A. 1997, *J. Geophys. Res.*, 102, 4719
 Kahler, S. 1994, *ApJ*, 428, 837
 Landau, L. D., & Lifshitz, E. M. 1959, *Fluid Mechanics* (Oxford: Pergamon)
 Lee, M. A. 1983, *J. Geophys. Res.*, 88, 6109
 Li, G., Zank, G. P., & Rice, W. K. M. 2003, *J. Geophys. Res.*, 108, 1082, doi: 10.1029/2002JA009666
 Ng, C. K., Reames, D. V., & Tylka, A. J. 1999, *Geophys. Res. Lett.*, 26, 2145
 ———. 2003, *ApJ*, 591, 461
 Powell, K. G., Roe, P. L., Linde, T. J., Gombosi, T. I., & DeZeeuw, D. L. 1999, *J. Comput. Phys.*, 154, 284
 Reames, D. V. 1999, *Space Sci. Rev.*, 90, 413
 ———. 2002, *ApJ*, 571, L63
 Roussev, I. I., et al. 2004, *ApJ*, 605, L73
 Skilling, J. 1971, *ApJ*, 170, 265
 Tylka, A. J. 2001, *J. Geophys. Res.*, 106, 25333
 Zank, G. P., Rice, W. K. M., & Wu, C. C. 2000, *J. Geophys. Res.*, 105, 25079